A GRAPHICAL AUTOMATED DETECTION SYSTEM TO LOCATE HARDWOOD LOG SURFACE DEFECTS USING HIGH-RESOLUTION THREE-DIMENSIONAL LASER SCAN DATA

Liya Thomas and R. Edward Thomas[1]

Abstract.—We have developed an automated defect detection system and a state-of-the-art Graphic User Interface (GUI) for hardwood logs. The algorithm identifies defects at least 0.5 inch high and at least 3 inches in diameter on barked hardwood log and stem surfaces. To summarize defect features and to build a knowledge base, hundreds of defects were measured, photographed, and categorized. Our cost-effective, reliable, and robust statistical method locates surface defects using a commercially available high-resolution laser scanner. The scanned data capture three-dimensional (3-D) images that illustrate log shapes—protrusions and depressions—and portray bark patterns. Most available optimization systems were designed to determine gross external characteristics (e.g., shape, diameter, sweep) of softwood logs. They then better position the log with respect to the saw and improve the sawyer's decision-making ability. Adding external defect information to the optimization process is a natural extension of current technology. Our method applies decision rules obtained from the knowledge base and identifies severe defects. Using the defect detection GUI, we tested our system. Using 14 randomly selected logs, we detected 53 severe defects out of 64. Nine nondefective regions were falsely identified. When defects were calculated as areas, 90.2 percent of defects were located.

INTRODUCTION

For decades hardwood log processing optimization methodologies and techniques have been one of the top priorities in the wood products industry (Chang 1992). After harvesting, a tree undergoes a rough manual estimation of potential yields and is bucked into several logs. Before a log is sawn into boards, the operator quickly examines it and picks the best opening or highest-quality face. During the inspection, surface defects are identified and types, severity, and topological distribution of defects determined. Thus, lumber yield is highly subject to time constraints and the operator's skills and conditions at the time. Defects, such as sawn-knot stubs, rotten knots, surface distortion, holes, cracks, branch sprouts, swelling, worm holes, and animal damage, are imperfections that decrease wood value.

There are two types of wood: softwood and hardwood. Most softwoods have a fast growth rate and identical, clustered defects mostly caused by branch pruning. Hardwood trees generally grow more slowly and the distribution of surface defects is random. Hardwood defects vary in size, shape, and type, making them difficult to identify. Internal defects exist inside the log, while external defects are visible on the tree or log surface.

[1]Research Faculty (LT), Concord University, Department of Math and Computer Science, Athens, WV 24712; Research Scientist (RET), U.S. Forest Service, Northern Research Station, Princeton, WV 24740. LT is corresponding author: to contact, call (540) 922-3822 or email at lhthomas@gmail.com.

With the advance of scanning equipment, it is possible to develop automated systems that aid bucking and sawing processes. Researchers have experimented with technologies and methods that locate and classify internal as well as external defects on either softwood or hardwood. Systems including those using X-ray/Computerized Tomography (CT), X-ray tomosynthesis, magnetic resonance imaging (MRI), microwave scanning, ultrasound, and ground-penetrating radar have been researched and developed to detect internal defects (Wagner and others 1989, Chang 1992, Guddanti and Chang 1998, Devaru and others 2005). Advanced computer vision and image-processing methods and algorithms were proposed for internal defect inspection on hardwood (Li and others 1996; Zhu and others 1996; Tian and Murphy 1997; Bhandarkar and others 1999). Some of these methods and technologies provide high detection rates as their data have extremely high resolution. However, issues such as high cost, low processing speed, data instability, and environmental safety keep them from being commercially available. Another approach is the use of laser scan technologies to collect profile data of softwood and hardwood logs. High-resolution 3-D laser-scanned data of hardwood logs show minute surface variations, making it feasible to detect external defects.

Compared to other systems such as X-ray/CT, laser-scanning equipment is more economical, safer, faster, and more suitable for log sizes (Thomas and others 2007). X-ray based systems might be appropriate for high-end veneer mills, if practical problems such as log size limitations can be resolved. External defect indicators are highly correlated with internal defect characteristics in hardwoods (Thomas 2008). This high correlation strongly suggests that automatically locating external defects based on laser-scanned data can help stem bucking and lumber sawing. In 2001, as the first group attempting external defect detection using laser-scanned log data, we began the development of a software system to identify and locate severe surface defects. Two batches of data were collected from two commercially important northeastern-American hardwood species, yellow-poplar (*Liriodendron tulipifera*), and northern red oak (*Quercus rubra*) (Fig. 1). To build a database, we measured, photographed, and categorized more than 200 external defect samples. Information was extracted from the database to develop the expert system in our defect detection algorithm.

A new robust statistical estimator was created to fit 2-D circles to data cross sections in the presence of severe outliers (Thomas and Mili 2007). Radial distances are computed between the virtual log made of fitted 2-D circles and log data, based on which computer vision techniques were applied to generate a gray-scale height image of the log surface. Contour curves also are generated that display ups and downs. The defect detection algorithm analyzes both contours and 3-D data to locate severe defects at least 0.5 inch high and 3 inches wide. Defective regions are selected and framed in rectangles over the contour plot. The algorithm was implemented in Java and Matlab on a Windows XP operating system (Thomas and others 2006) and has been merged in Java. A state-of-the-art Java GUI was developed that allows users to control the log scanner, to scan log data, to execute our detection system, and to display detection results. Using the defect detection GUI, we tested the system.

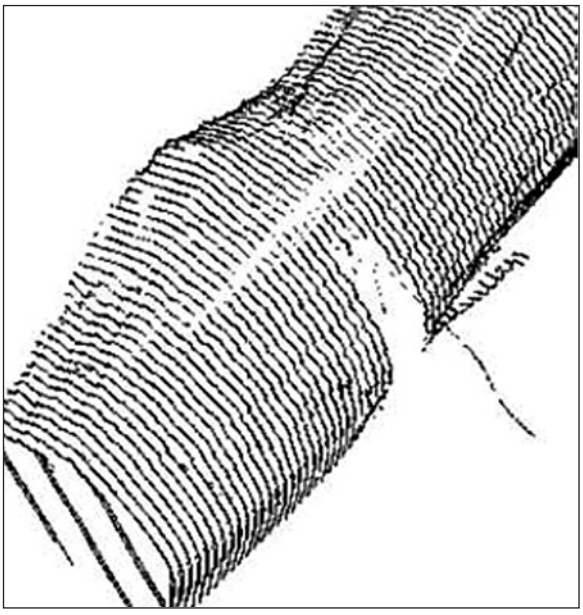

Figure 1.—Portion of the 3-D projection of laser-scanned range data for a red oak log.

STUDY AREAS

Our log-surface defect detection algorithm processes gray-scale imagery and 3-D range data by using a new robust generalized M-estimator, or GME (Thomas and Mili 2007). It extracts radial distances between the virtual log formed by a series of fitted circles and log data points. The radial distances provide a height map of the log surface with respect to the virtual log. This mapping enables our system to locate defects associated with unique characteristics and height change. Wagner and others (1989) experimented with a CT scanner operating at a speed acceptable to mills that collected internal log images for automatic defect detection. Using X-ray/CT images, Guddanti and Chang (1998) constructed virtual boards to resemble real sawn boards that demonstrated the feasibility of applying the technique. Zhu and others (1996) developed an inspection algorithm to identify internal log defects in CT images. It comprises an adaptive filter, a multi-threshold 2-D segmentation scheme, and a 3-D 8-neighbor connectivity analysis mechanism.

Using CT technology, Li and others (1996) investigated internal log inspection and developed a feed-forward multilayer Artificial Neural Network (ANN) system, trained by back propagation. It can classify three common defect types—knots, splits, and decay—and can accommodate several hardwood species, including northern red oak, water oak (*Q. nigra* L.), yellow-poplar, and black cherry (*Prunus serotina*). Local 3-D data are used to extract defect features, and a pixel-by-pixel classification accuracy of 95 percent was achieved. Sarigul and Abbott (2000) further refined these classifiers in a subsequent post-processing step, and developed the Intellipost system using domain-dependent rules. It improved segmentation accuracy of Li and others (1996) ANN by 1.92 percent, 9.45 percent, 4.22 percent, 0.33 percent for a red oak dataset, datasets provided by Forintech Canada, Inc., and two medical ones, respectively. Bhandarkar and others (1999) developed the CATALOG system for internal defect detection and classification via CT image analysis, consisting of segmentation and correlation phases. Hardwood species studied were red oak, black walnut (*Juglens nigra*), white ash (*Fraxinus americana* L.), and hard maple (*Acer saccharum*). Recent research activities in internal hardwood defect detection by X-ray/CT imaging include a group in Purdue University (Callahan 2007). Tian and Murphy (1997) proposed an automated digital camera-based texture analysis system, KnotVision, to locate and identify defects on freshly harvested pine logs (softwood).

Strong relationships among surface indicators and internal defect features have been discovered for severe defects, such as overgrown knots, sound knots, knot clusters, and unsound knots (Thomas 2008). For example, the strength of the correlations (adjusted multiple R^2) between interior halfway-point width measurement and exterior features ranged from 0.48 to 0.75. Similar results were found between external features and the halfway-point length measurement (adjusted multiple R^2 from 0.45 to 0.75). All correlations between external indicators and internal features were significant at the 99-percent level. Further, the low mean absolute errors (0.25 to 0.70 inch) indicate that internal features can be reliably predicted using external defect measurements. The defect detection algorithm discussed here identifies the size and location of surface defects. When this information is passed to the internal defect prediction model (Thomas 2008), a complete set of defect information for a log, internal and external, is generated. This is the data necessary to optimize the processing of the log to yield maximum product value. A recent test of the internal prediction models has shown that they can accurately predict the occurrence of 80 percent of the knots on sawn board faces.

METHODS

The fact that external defects corresponding to rises or depressions on log surface can be observed from 3-D range images suggests that defect locations can be determined by extracting surface height from the images. Three major steps are involved.

1) Fit 2-D circles to log cross-sections. Because datasets might have missing data or include irrelevant, deviant data points, a new, robust estimator was developed to estimate in a reliable manner the centers and radii of the fitted circles.
2) Extract radial distances between circles and log data to indicate local height changes. Radial distances refer to height values on the surface with respect to the reference.
3) Locate defects characterized by significant surface rises or depressions.

We experimented with methods that fit circles and ellipses to log data to create a reference surface, or virtual log, for converting 3-D data to 2-D images for processing. Our GM estimator that fit circles to the cross-section data showed little to no influence from the outlier data (approximately 3 percent of the dataset) or the missing data (Fig. 2). Our process converts 3-D range data to radial distances and uses image-processing methods commonly applied to gray-scale values (Fig. 3a). In this process, the log surface is unrolled onto a 2-D coordinate space to create a "skin" representing the pattern of log bark along with bumps and bulges associated with most defects. Radial distances are calculated between circle and log surface points, typically ranging from –0.5 to 0.5 inch, scaled to range from 0 to 255 gray-levels, and mapped to create a 2-D image. Log data are processed and interpolated linearly to fill any gaps between data points to form a grid. In our original data set, the cross-sectional density is nearly 20 times the longitudinal density, and linear interpolation generates an image proportional to the real log surface.

Six contour levels are computed from the orthogonal distances between a virtual log and any point of the cross section, generating a topographical exterior log map. Examining only the highest-level and lowest-level contours, we can detect defects corresponding to surface rise or depression. Log data also are referenced to find defects. Expert knowledge, in the form of defect shape and size characteristics, is applied in a stepwise fashion to rule out regions as potential defects, including regions with sizes smaller than a given threshold, nested in other curves, or long and narrow (determined by the actual width-to-length ratio of real log dimensions). The algorithm was created under the assumption that data resolution is 0.8 inches per cross section, so only those with a relatively significant height change on the surface (at least 0.5 inch), and/or a relatively significant size (at least 3 inches in diameter) are examined. Using radial distances visualized by the gray-level image in Figure 3a, the algorithm generates a contour plot as depicted in Figure 3b,

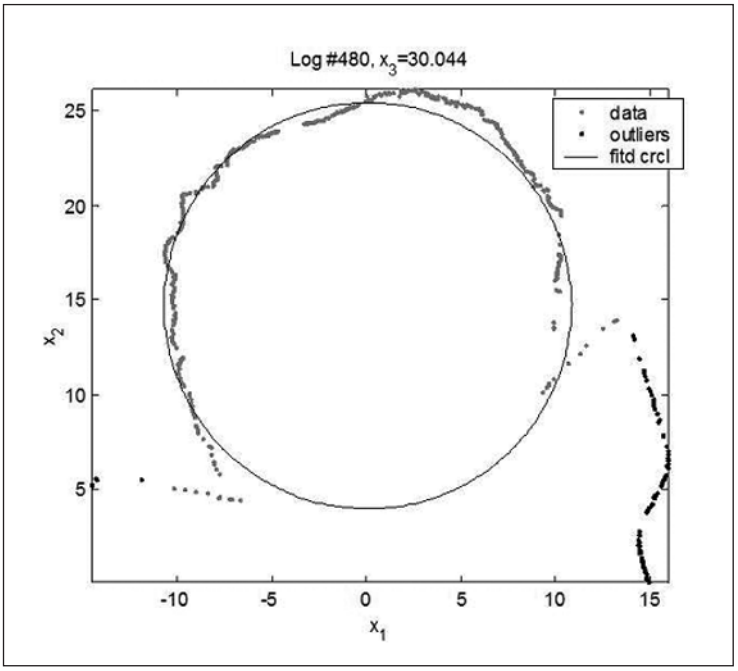

Figure 2.—Circle fitting to a cross section with severe outliers as a portion of the log support.

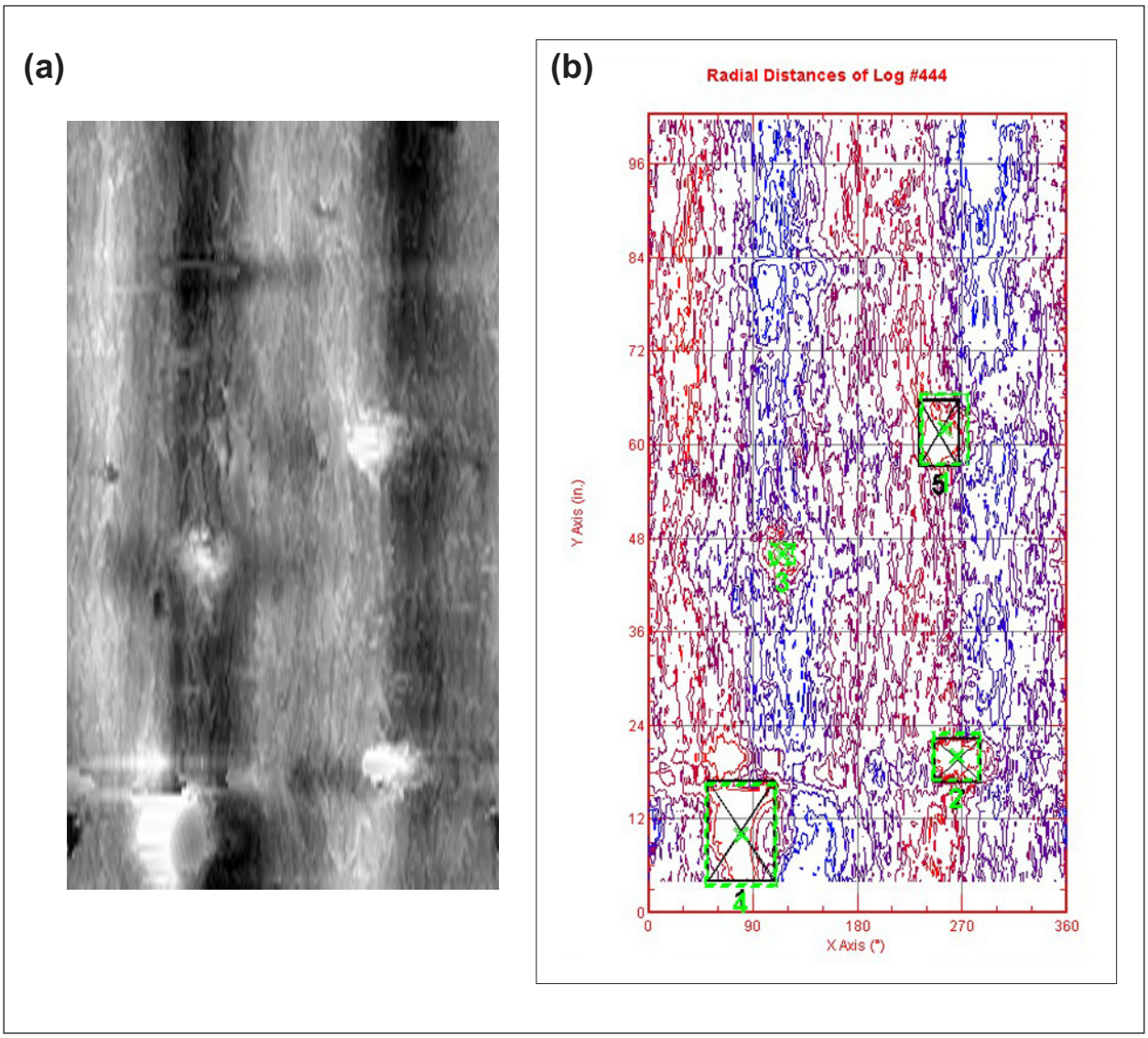

Figure 3.—(a) Radial distances generated by the log-unrolling process presented as a gray-level range image. Lower-left corner has a sawn knot, where sawn pattern can be observed. (b) Three out of four defects are automatically detected as displayed in the contour plot, enclosed in black crossed rectangles. The only exception is in the top left corner. Also shown is a manually recorded map of defects on the same log, enclosed in light green rectangles centered by a small cross.

and determines rectangle-enclosed regions bounding contour curves at the highest level. Some regions are selected if they are big enough or with a significant height.

The detection method uses a statistical procedure to examine the region surrounding a selected small region for relatively straight-line segments (Hampel et al. 1986). If the coverage of straight-line segments is sufficient, the defect region is adjusted to cover the entire defect surface, rather than just a corner. Such a region is identified as a flattop, which is likely a sawn top, either sound (not rotten), or unsound (rotten). Region-removal rules are given as follows: regions smaller than a given threshold; regions enclosed in curves nested in other curves, as there will be at most one defect in the same location; long and narrow regions (because they are normal bark regions); regions that are smaller than 50 in^2 and are too close to the selected large ones. Some

regions are removed for further consideration if they contain a large portion of missing data. The algorithm extends boundaries of an identified region if only a relatively high standing corner of the defect is located. Regions may include elevated yet nondefective log surface. Typically they are covered with tree bark and are thus associated with distinctive bark patterns.

RESULTS

Two groups of data were collected for our experiment. The first, scanned using a Perceptron scanning system (Perceptron Inc., Plymouth, MI), consists of more than 160 log data samples from both species, each with cross sections along the log length at 0.8-inch intervals and a resolution of about 0.04 inch within a cross section, shown in Figure 1. Each log data sample in this group consists of approximately 120,000 to 240,000 points (3-D coordinates). The second group was scanned using a JoeScan system (JoeScan, Vancouver, WA). It contains more than 140 red oak data samples, with a resolution of 0.06 inch between cross sections, and 0.09 inch within a section. The number of cross sections per log ranges from 1,600 to 3,200, and each cross section has 400 to 800 points. Thus, the second data group has much higher resolution and number of data points varies from 0.64 to 2.56 million per log sample. The prototype of our defect detection system was created and tested using the first data. The circle-fitting part in the algorithm was implemented using Java. The rest of the algorithm that detects defects based on radial distances was written in MATLAB 7.0 (MathWorks, Natick, MA; MATLAB 2008) for its readily available and easy-to-use graphical capabilities.

To make our system easier to use, a sophisticated graphical interface was developed that allows users to enter various information by selecting items through pull-down menus, then to run it by pressing a button (Fig. 4). Through the interface, a user may control the scanning process of the log scanner and launch the log

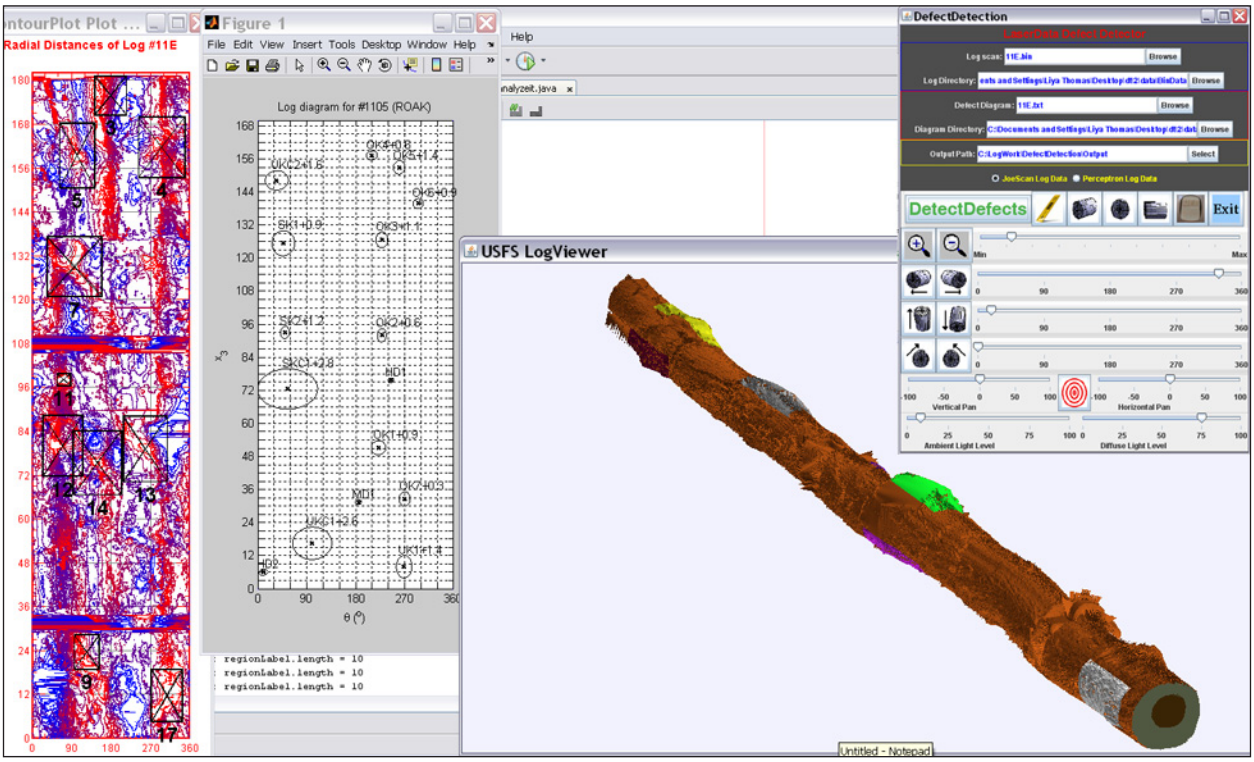

Figure 4.—Partial screen shot of GUI (Graphical User Interface) for the defect detection system. On the left side is the contour plot with automatically detected regions enclosed in black crossed rectangles. To the upper-right is the control panel.

data scan. Once the data are collected, the user may press the corresponding button to execute our detection system. Detection results are automatically displayed in three different forms: a 3-D projection of the log data with defective regions marked; a contour plot tiff image of the log surface height change, also with defective region marked; and a text file of residual values. The 3-D log data projection can be viewed interactively. The user can zoom in/out, rotate, or pan it. Lighting also can be adjusted. These capabilities make our system both interactive and real-time.

We used an open-source Java package to generate 2-D contour plots of data (Huwaldt 2002). Figure 3b presents a contour plot with automated defect detection results overlaid by observed severe defective regions. Changes were made to the Huwaldt package to accommodate our detection system and fix several incompatibilities. Huwaldt's package was developed for relatively small datasets, while the log data can have as many as 2.5 million 3-D points. Thus, we reduced the data to 50 percent for the first group and 17 percent for the second one; that is, 90,000 and 272,000 points on average, respectively. Resolutions for the two groups are 0.8×0.08 in^2/pixel, and 0.2×0.2 in^2/pixel, respectively. To get a uniform resolution along both the log length and cross section in the first batch, linear interpolation was performed in the direction of log length. Data reduction ensures that the current version of our system will complete the analysis within a reasonable amount of time. This processing speed is possible because a data mesh with these densities is fine enough for a contour-curve based detection algorithm such as ours that aims only at the most protruding regions.

Tables 1 and 2 show simulation results from 14 log samples from the Perceptron data using our new Java implementation. Out of 64 severe defects, we detected 53. We falsely identified nine nondefective regions. When defective regions are calculated as areas, 90.2 percent of the defects were located and 1.8 percent of the total clear area falsely identified as defective. The algorithm made the assumption that data resolution is no more than 0.8 inch per cross section (along log length), which confines the defect size that can be detected to be no more than 3 inches wide, and at least 0.5 inch high. Otherwise there would be fewer than four cross sections spanning a defect, and low-lying defects are not enclosed in the highest-level contours, usually at

Table 1.—Defect detection simulation results in terms of number of rectangle regions for 14 log samples.

Log #	Total	Detected	Missed	False
444	4	3	1	-
448	8	7	1	1
450	4	3	1	-
453	7	6	1	-
468	3	3	-	-
480	5	5	-	1
493	5	3	2	-
501	3	3	-	-
508	5	4	1	1
521	6	5	1	4
537	4	3	1	-
441	2	2	-	-
485	6	4	2	1
520	2	2	-	1
Sum	64	53	11	9

Table 2.—Defect detection simulation results in terms of area (in²) for 14 log samples.

Log #	Surface	Observed	Detected	Missed	False
444	5,797	215	187	8	-
448	7,284	805	812	24	217
450	7,278	235	326	15	-
453	6,301	1,168	928	36	-
468	5,453	812	949	-	-
480	7,486	798	750		166
493	8,551	255	299	42	-
501	3,916	466	387	-	-
508	4,031	459	532	30	295
521	8,560	720	596	24	414
537	6,414	389	263	23	-
441	4,645	202	207	-	-
485	9,352	1,126	715	288	272
520	6,188	368	282	-	159
Total	91,256	8,018	7,233	490	1,523
%	-	-	90.2	6.1	1.8

about 1 inch. The resolution of the second batch is five times higher than that of the first one—0.06 × 0.1 in²/pixel vs. 0.8 × 0.04 in²/pixel. Thus, it is possible to identify defects at the higher resolution that were not previously identified.

We are testing our detection system with both groups of data. During testing with JoeScan data, several problems appeared. First, the algorithm is an expert system that uses many parameters, for example, region width and height, as a threshold to rule out selected regions that are not defective. At places, these parameters are examined using number of points within a cross section, which depends on resolution . Second, due to a data collection issue, noise appears frequently with the higher-resolution data. Third, data resolution along cross sections in the second batch appears to vary. These shortcomings interfere with detection results and more tuning is needed to improve detection capability and reduce false rates. Execution time per log sample is less than 1 minute with data from the Perceptron scanner, and about 1.2 minutes with data from the JoeScan scanner on a desktop computer with an Intel 2.6 GHz Core2 processor.

DISCUSSION

Other than the severe defects that our system is able to identify, there are other groups of severe defects such as heavy distortion (HD) and mild distortion (MD). They are not associated with significant size (mostly about 2-3 inches in diameter), or height change (less than 1 inch high). In a 2007 study of red oak, we counted defect numbers for all defects, all logs, and all trees (Thomas et al. 2007). We identified 1,376 surface defects, among which 60 are HDs, and 103, MDs. They represent 4.4 percent and 7.5 percent of all defects, respectively. Although they lack the topological characteristics of other severe defects, HDs and MDs typically present unique bark patterns. We are looking into technologies such as computer pattern recognition to locate them. From the gray-scaled surface-rise images of 64 third and higher red oak logs with which we experimented, only 12 HDs and 1 MD were at all visible to the human eye. Locating HDs and MDs by computer software is likely difficult, as software will be developed by researchers, in a sequence of programming commands. Obviously it is going to be much more limited than the processing power of

the human brain. Further, the only thing our detection system has to work with is surface height images. Currently it cannot get help from digital color images or from ground truth. With limited input information and limited capability, it remains unknown how effective the detection module can be for defects that include HDs and MDs.

Much can be improved in our defect detection algorithm. Problems arose due to different data resolution. Parameters should be redefined to accommodate different data resolutions—although given the current structure, such modification to the system likely requires a complete overhaul. Currently the contour plot package is built upon JFrame, a Java primitive class. The quality of the resulting plots is not desirable. Adjusting, editing, and storing the graphs are inconvenient, making analysis of results difficult. We shall experiment with other graphical representation methods to improve graphical quality. Further, pattern recognition and neural network methods will be investigated for detecting severe defects without significant height changes, but with unique bark patterns. This application can be observed in Figure 3a where, in the lower-left corner, the sawn pattern is displayed in the radial distance image.

We have tested our system with more data. Our new GUI is easier to navigate and more user-friendly to sawmill operators. The detection software is integrated with the laser scanning system. Lab experiments were conducted to integrate and test the system using sample logs. We are collaborating with a sawmill located in West Virginia to perform real-time industrial testing. We hope our defect detection system will eventually provide a tool that is both effective and affordable for the forest products industry.

ACKNOWLEDGMENT

This research was funded in part by a grant from the Wood Education Resource Center, Princeton, WV.

LITERATURE CITED

Bhandarkar, S.; Faust, T.; Tang, M. 1999. **Catalog: a system for detection and rendering of internal log defects using computer tomography.** Machine Vision and Applications. 11(4): 171-190.

Callahan, R. 2007. **Scientists test CT scanners on trees.** USA Today. [online]. Available: http://www.usatoday.com/tech/science/2007-06-08-3237455238_x.htm.

Chang, S. 1992. **External and internal defect detection to optimize cutting of hardwood logs and lumber.** Transferring Technologies for Industry No. 3. Beltsville, MD: U.S. Department of Agriculture, National Agriculture Library. 24 p. Available: http://www.nal.usda.gov/ttic/industry/ hrdwood3.htm. [Date accessed unknown.]

Devaru, D.; Halabe, U.B.; Gopalakrishnan, B.; Agrawal, S.; Grushecky, S. 2005. **Algorithm for detecting defects in wooden logs using ground penetrating radar.** SPIE (5999): 59990B.

Guddanti, S.; Chang, S. 1998. **Replicating sawmill sawing with topsaw using CT images of a full length hardwood log.** Forest Products Journal. 48(1): 72-75.

Hampel, F.; Ronchetti, E.; Rousseeuw, P.; Stahel, W. 1986. **Robust statistics: the approach based on influence functions.** New York, NY: John Wiley. 528 p.

Huwaldt, J. 2002. **Plot Package, jahuwaldt.plot.** [online]. Available: http://homepage.mac.com/jhuwaldt/java/Packages/Plot/PlotPackage.html. [Accessed 10 May 2008].

Li, P.; Abbott, A.; Schmoldt, D. 1996. **Automated analysis of CT images for the inspection of hardwood log.** In: Proceedings IEEE conference on neural networks. Washington, DC. 3: 1744-1749.

MATLAB – The language of technical computing. 2008. [online]. Available: http://www.mathworks.com/products/matlab/. [Cited 10 May 2008].

Sarigul, E.; Abbott, A.; Schmoldt, D. 2000. **Rule-driven defect detection in CT images of hardwood logs.** In: Proceedings of the 4th international conference on image processing and scanning of wood: 37-49.

Thomas, L.; Mili, L. 2007. **A robust GM-estimator for the automated detection of external defects on barked hardwood logs and stems.** IEEE Transactions on Signal Processing. 55(7): 3568-3576.

Thomas, L.; Mili, L.; Thomas, E.; Shaffer, C. 2006. **Defect detection on hardwood logs using laser scanning.** Wood & Fiber Science. 38(4): 682-695.

Thomas, L.; Shaffer, C.; Mili, L.; Thomas, E. 2007. **Automated detection of severe surface defects on barked hardwood logs.** Forest Products Journal. 57(4): 50-56.

Thomas, R.E. 2008. **Predicting internal yellow-poplar log defect features using surface indicators.** Wood & Fiber Science. 40(1): 14-22.

Tian, X.; Murphy, G. 1997. **Detection of trimmed and occluded branches on harvested tree stems using texture analysis.** International Journal of Forest Engineering. 8(2): 65-78.

Wagner, F.; Taylor, F.; Ladd, D.; McMillin, C.; Roder, F. 1989. **Ultrafast CT scanning of an oak log for internal defects.** Forest Products Journal. 39(11/12): 62-64.

Zhu, D.; Conners, R.; Schmoldt, D.; Araman, P. 1996. **A prototype vision system for analyzing CT imagery of hardwood logs.** IEEE Transactions on Systems, Man, and Cybernetics Part B: Cybernetics. 26(4): 522-532.